Nonlinear Model Predictive Control For Circadian Entrainment Using Small-Molecule Pharmaceuticals

John H. Abel * **Ankush Chakrabarty** ** **Francis J. Doyle III** **

* *Department of Systems Biology, Harvard Medical School, Boston, MA 02115, USA*
** *Harvard John A. Paulson School of Engineering and Applied Sciences, Harvard University, Cambridge, MA 02138, USA*

Abstract: Recent *in vitro* studies have identified small-molecule pharmaceuticals effecting dose-dependent changes in the mammalian circadian clock, providing a novel avenue for control. Most studies employ light for clock control, however, pharmaceuticals are advantageous for clock manipulation through reduced invasiveness. In this paper, we employ a mechanistic model to predict the phase dynamics of the mammalian circadian oscillator under the effect of the pharmaceutical under investigation. These predictions are used to inform a constrained model predictive controller (MPC) to compute appropriate dosing for clock re-entrainment. Constraints in the formulation of the MPC problem arise from variation in the phase response curves (PRCs) describing drug effects, and are in many cases non-intuitive owing to the nonlinearity of oscillator phase response effects. We demonstrate through *in-silico* experiments that it is imperative to tune the MPC parameters based on the drug-specific PRC for optimal phase manipulation.

Keywords: Biological control, model predictive control, circadian oscillator, phase response curve, time-varying weights

1. INTRODUCTION

Circadian rhythms are endogenous, near-24 hour oscillations in gene expression or metabolism driving temporal adaptations in most organisms. In mammals, these oscillations are generated by genetic feedback loops within each cell of the organism, and coordinated by a "master pacemaker" set of neurons in the hypothalamus (Mohawk et al. [2012]). Environmental signals, especially light, set the time of this biological clock. Mistimed environmental cues may result in a damping of these rhythms, and a loss of temporal regulation of genetic architecture.

Chronic disruption to the circadian clock such as rotating shift work and chronic jet lag has been associated with psychological and physiological pathologies (Marquié et al. [2015]). In recent years, small-molecule pharmaceuticals have gained significant interest as a path toward modulating the circadian clock to reduce the effects of circadian disturbances (Hirota et al. [2010, 2012]). Small-molecule pharmaceuticals present advantages over the use of light for clock resetting, including avoiding the daytime light "dead-zone" where there is little phase response to light, and reducing the burden on the individual to tightly control their light environment. Light-based approaches, for example, would necessitate wearing low-transmission glasses or a light visor for extended time periods (Serkh and Forger [2014]). Furthermore, light dosing strategies may take several days to complete, hence the prevalence of jet lag following long trips. Pharmaceuticals are expected to enable direct manipulation of sensitive control targets, allowing more rapid clock resetting (Bagheri et al. [2008]). The complex nature of the circadian oscillator necessitates a control approach toward dosing strategies for these drugs, as an identical stimulus applied at different times of day may have drastically different effects on the clock. Additionally, modeling approaches such as those reported in St. John et al. [2014] have been employed to identify the underlying mechanistic action of these drugs. These models may, in turn, be used to exert control over the clock.

Prior studies have developed simple optimal control or MPC approaches toward manipulating the circadian clock. Bagheri et al. [2007, 2008] first demonstrated MPC and multi-target MPC for light-resetting a *Drosophila* circadian clock model, and suggested identifying control targets by choosing complementary phase response curves (PRCs). Slaby et al. [2007] and Shaik et al. [2008] used optimal control approaches to phase shift a *Drosophila* clock model, and simplified the computation of the optimal control trajectory via reduction to a mixed-integer optimal control problem. Zhang et al. [2016] used light-based optimal and feedback control to investigate re-entrainment of a human clock model, and also devised a strategy for identifying the optimality of the singular arcs resulting from this singular control problem. Serkh and Forger [2014] also developed light-based optimal control, and reduced the computational complexity of the problem by searching for switching times for bang-bang light schedules. Optimal control approaches may suffer significantly for a noisy system or due to plant-model mismatch, and remain computationally prohibitive, if not intractable, for complex high-dimensional nonlinear models (Shaik et al.

[2008]). MPC presents a potential path toward reducing the complexity of the control problem while providing inherent robustness to noise and plant-model mismatch. However, identification of design principles for circadian applications of MPC remains a relatively unexplored problem.

Herein, we present a novel approach to manipulating the clock via nonlinear MPC by optimally dosing the small-molecule pharmaceutical, KL001 (Hirota et al. [2012]). We expand upon the simplistic proof of concept demonstrated in Abel and Doyle III [2016] to identify necessary considerations for the successful application of MPC to this problem. Specifically, we demonstrate, via extensive simulations, the need to select appropriately long predictive horizons and appropriately short controller sampling times to exploit the phase response properties of the circadian clock and rapidly control re-entrainment.

The paper is organized as follows: in Section 2.1 we introduce a well-established mechanistic limit cycle model of the mammalian circadian clock, used as the plant in this study. In Sections 2.2 and 2.3, we formulate the MPC problem in a novel fashion by reducing this 8-state dynamic model of the circadian clock to its phase-only (1-state) form, with phase response to KL001 governed by the parametric phase response curve derived from the full model. We then use the parametric infinitesimal phase sensitivity of the model to attain a linear approximation of the KL001 dose-dependent phase response. In Section 3.1, we show that this simplified model may be used within MPC to re-entrain the clock following phase shifts in the environment. In Sections 3.2 and 3.3, we perform extensive simulations to examine predictive horizon and controller sampling time, and demonstrate that naively selecting these parameters could result in significant degradation of controller performance.

2. PROBLEM FORMULATION

2.1 Dynamical circadian model

Circadian rhythms are generated within individual cells by a negative genetic feedback loop in which isoforms of the genes *Period* (*Per*) and *Cryptochrome* (*Cry1*, *Cry2*) are transcribed, translated, form dimers, and repress their own transcription. These dimers are then degraded, and the cycle repeats itself. Numerous models of this gene network have been proposed; most often these models are formulated as deterministic limit cycle oscillators (Leloup and Goldbeter [2003]; Kronauer et al. [1999]). Fig. 1A shows the dynamic states and reactions in the limit cycle oscillator model that simulates the dynamics of KL001. For the full set of model equations and parameters, we refer the reader to St. John et al. [2014]. This model includes *Per*, *Cry1*, and *Cry2* mRNAs; PER, CRY1, and CRY2 cytosolic proteins; and PER-CRY1 and PER-CRY2 nuclear transcription factors with a total of 8 ODEs and 21 kinetic parameters.

KL001 stabilizes nuclear CRY by reducing the degradation rate of nuclear PER-CRY1 and PER-CRY2 as identified in St. John et al. [2014]. Thus, the model equations describing the dynamics of PER-CRY dimers (C1P and C2P) are modified to become:

$$\frac{d\mathrm{C1P}}{dt} = v_{\mathrm{a,CP}}\mathrm{P}\cdot\mathrm{C1} - v_{\mathrm{d,CP}}\mathrm{C1P} - \frac{(vdCn - u(t))\mathrm{C1P}}{k_{\mathrm{deg,Cn}} + \mathrm{C1P} + \mathrm{C2P}} \tag{1a}$$

$$\frac{d\mathrm{C2P}}{dt} = v_{\mathrm{a,CP}}\mathrm{P}\cdot\mathrm{C2} - v_{\mathrm{d,CP}}\mathrm{C2P} - \frac{(vdCn - u(t))m_{\mathrm{C2N}}\mathrm{C2P}}{k_{\mathrm{deg,Cn}} + \mathrm{C2P} + \mathrm{C1P}}, \tag{1b}$$

where $u(t) \in [0, \bar{u}]$ is the control input, and $vdCn$ is the parameter that is reduced by KL001. The full set of model equations and parameterization is given in St. John et al. [2014].

Each unique point on the limit cycle solution $\mathbf{x}^\gamma$ may be assigned a unique phase $\phi \in [0, 2\pi)$. Any point not on the limit cycle (with the exception of the phase singularity point at the center of the limit cycle) may similarly be assigned the phase of the point on the limit cycle to which that point ultimately converges.

Remark 1. An oscillator at point $\mathbf{x}_a$ not on the limit cycle trajectory $\mathbf{x}^\gamma$ will converge to $\mathbf{x}^\gamma$ asymptotically in time. We then define the phase $\phi(\mathbf{x}_a) \in [0, 2\pi)$ as the phase of the oscillator on $\mathbf{x}^\gamma$ to which the oscillator at $\mathbf{x}_a$ will ultimately converge. That is,

$$\phi(\mathbf{x}_a) = \arg\min_{\phi} \lim_{t\to\infty} ||\mathbf{x}(t) - \mathbf{x}^\gamma(t-\phi)||,$$

where $\mathbf{x}(0) = \mathbf{x}_a$.

Since we are primarily interested in the phase of oscillation rather than the state concentrations, the 8-state model

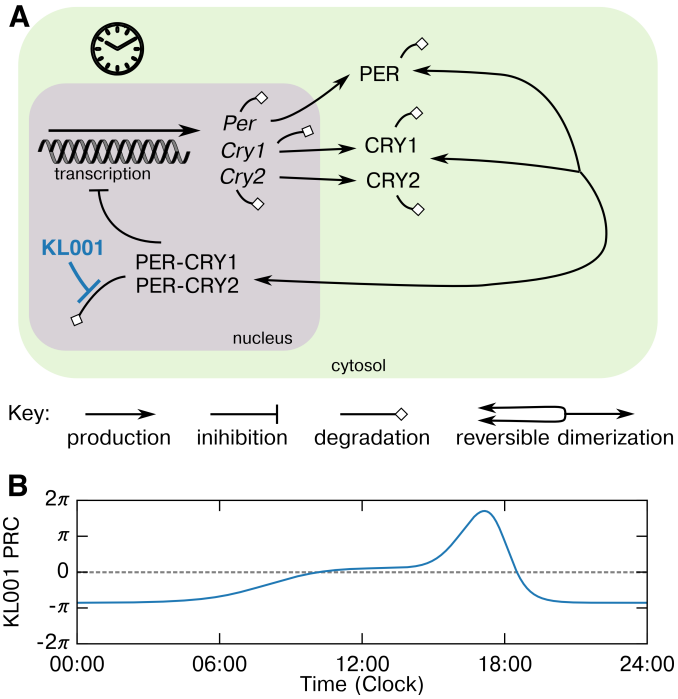

Fig. 1. Schematic of the core circadian gene network and effect of KL001. (A) The core circadian negative feedback loop. KL001 stabilizes nuclear CRY by reducing its degradation rate, as shown in blue. (B) Parametric infinitesimal phase response curve (PRC) for KL001-mediated stabilization of nuclear CRYs.

of St. John et al. [2014] may be reduced to a single ODE describing the phase dynamics of the model (Taylor et al. [2008a]). To capture the response of the oscillator to KL001, this phase-only representation must be modified with the parametric phase response curve, which is derived from the full 8-state model.

2.2 Problem statement

The aim of this paper is to design a nonlinear MPC that recommends dosing strategies to facilitate rapid re-entrainment following an environmental phase shift. We denote the phase of the external environment $\phi_e \in [0, 2\pi)$, and the phase of the circadian oscillator $\phi \in [0, 2\pi)$. The phase dynamics of the oscillator is given by:

$$\frac{d\phi}{dt} = \frac{2\pi}{\tau} + f(u(t)), \tag{2}$$

where τ is the intrinsic oscillator period (set to 24h) and $f(\cdot)$ is a nonlinear function that describes the phase response to the bounded control input $u \in [0, \bar{u}]$; we will elaborate upon $f(u(t))$ in the following subsection.

The phase of the external environment follows the dynamics:

$$\frac{d\phi_e}{dt} = \frac{2\pi}{\tau_e} + \Delta\phi\, \delta(t_{\text{shift}}),$$

where τ_e is the intrinsic environmental period (also set to 24h), and $\Delta\phi : \mathbb{R} \to [0, 2\pi)$ denotes an instantaneous phase shift at time $t_{\text{shift}} \in \mathbb{R}$. We assume that the circadian oscillator begins in an entrained state, that is, $\phi_e(0) = \phi(0)$. This assumption is realistic, as a human is entrained in standard daily conditions.

Remark 2. Phase of the oscillator and the environment is 2π-periodic. Thus, a phase advance of π and a phase delay of $-\pi$ are considered equivalent (alternately, a phase advance of $\pi/2$ is equivalent to a delay of $-3\pi/2$, etc.).

Formally, our objective is to determine an optimal trajectory of admissible control actions that entrains the phase of the oscillator ϕ to the phase of the environment ϕ_e. Specifically, we seek a piecewise constant admissible control trajectory $u^\star : [t_{\text{shift}}, \infty) \to [0, vdCn]$ that satisfies

$$\lim_{t\to\infty} \|\phi(t, u) - \phi_e(t)\| = 0.$$

We describe the function f next.

2.3 Exploiting the phase response curve for computing MPC

To compute $f(u(t))$ from (2), we approximate the phase response to perturbation as linear in both time and parameter change using the parametric infinitesimal phase response curve (PRC) given by $\frac{d}{dt}\frac{d\phi}{dp}$. The PRC describes how the phase of the oscillator is affected by an infinitesimal change in parameter p for an infinitesimal time. Here, p is the kinetic parameter $vdCn$, and the $d(vdCn)$ term is negative to reflect the reduction in this parameter. This PRC is calculated numerically from the full 8-state model using sensitivity analysis as in Taylor et al. [2008b], and may be used to in conjunction with (2) to describe the phase dynamics of the oscillator:

$$\frac{d\phi}{dt} = \frac{2\pi}{\tau} - u(t)\,\Gamma(\phi), \tag{3}$$

where

$$\Gamma(\phi) = \frac{d}{dt}\frac{d\phi}{d(vdCn)}.$$

Since this formulation is a linear approximation of the phase response calculated for points on the limit cycle, it implicitly assumes that all points with the same phase respond identically to the same stimulus regardless of where they lie in state space. Thus, the local linear approximation is developed only once, and solved simultaneously for all points that lie on the limit cycle using the methods described in Abel and Doyle III [2016]. This assumption holds for cases sufficiently close to the limit cycle, but fails notably near the singularity. The parametric infinitesimal PRC is plotted in Fig. 1B.

Recall that the control action $u(t)$ is bounded on $[0, \bar{u}]$. The maximal value $\bar{u}$ is set to the value of $vdCn = 0.101$ to conform to physical reality (i.e., slowing the rate of a reaction cannot reverse its direction).

Remark 3. Since $u(t)$ is non-negative, the phase ϕ can only be shifted in one direction along the PRC at any point in time.

Unlike light-based control, where the control input is near-instantaneous, pharmacokinetics necessitate a piecewise-constant parameterization of the control over which the drug levels may be chosen. This piecewise-constant parameterization renders the resulting continuous-time problem computationally tractable by converting the infinite-dimensional optimization problem to a finite-dimensional one.

Let the controller sampling time be denoted τ_u. Thus, the control trajectory is parametrized as:

$$u(t) = u(t_k) \tag{4}$$

for $t_k \le t < t_{k+1}$, where k denotes the sampled time instant when the control signal is updated. Note that $t_{k+1} - t_k = \tau_u$.

To estimate the phase of the oscillator ℓ samples (or, $\ell\tau_u$ hr) into the future, we integrate the PRC dynamics in (3), which yields

$$\hat{\phi}(t_k + \ell\tau_u) = \phi(t_k) + \frac{2\pi\ell\tau_u}{\tau} - \sum_{j=1}^{\ell} \int_{t_{k+j-1}}^{t_{k+j}} u(t_j)\Gamma(\phi)\, dt, \tag{5}$$

where $\hat{\phi}$ denotes the phase estimate and the control signal u has been parameterized as in (4).

Remark 4. Note that the approximation of phase in (3) has been investigated extensively in [Taylor et al., 2008b, Section 4]. Note also that our piecewise constant parametrization of the control trajectory does not approximate the phase dynamics as a discrete-time system, and so critical information obtained by the integration in (5) is not lost due to discretization effects.

Let N_p denote the predictive horizon of the MPC. Let

$$U \triangleq [u(t_k)\ u(t_k + \tau_u)\ \cdots\ u\,(t_k + (N_p - 1)\tau_u)]^\top \tag{6}$$

denote the control actions at the knots of the piecewise constant controller $u(t)$ over the predictive horizon. Also, let the corresponding deviations from environmental phase be denoted by

$$e_\phi(\cdot) \triangleq \left|\hat{\phi}(\cdot) - \phi_e(\cdot)\right|_{[0,2\pi)} \tag{7a}$$

and

$$g_\phi(\cdot) \triangleq \begin{cases} 0 & \text{if } e_\phi(\cdot) < \delta \\ e_\phi(\cdot) & \text{otherwise} \end{cases}, \tag{7b}$$

where $\hat{\phi}(\cdot)$ is obtained using (5), and $|\cdot|_{[0,2\pi)}$ is a modulo-2π function.

Remark 5. Here, δ is a tunable parameter below which the system is considered to be practically entrained. We have selected $\delta = 0.1$ (or a phase difference of approximately 20 minutes) for this application. As the error in calculating oscillator phase is $\mathcal{O}(10^{-2})$, this bound prevents the controller from taking unnecessary action resulting from numerical imprecision.

In order to obtain the sequence of KL001 doses, we solve, at each time instant t_k, the following finite-horizon optimal control problem:

$$u^\star = \arg\min_U \ \mathcal{J}$$

subject to:

$$\hat{\phi}(t_k + \ell\tau_u) = \phi(t_k) + \frac{2\pi\ell\tau_u}{\tau} - \sum_{j=1}^{\ell} \int_{t_{k+j-1}}^{t_{k+j}} u(t_j)\Gamma(\phi)\, dt$$

$$\mathcal{J} = \sum_{\ell=0}^{N_p-1} w_{\ell+1}^{\phi} g_\phi^2(t_k + (\ell+1)\tau_u) + w_\ell^u u^2(t_k + \ell\tau_u), \tag{8}$$

$$0 \le u_\ell \le \bar{u},$$

for all $\ell = 0, \cdots, N_p - 1$, where w_ℓ^u and $w_{\ell+1}^{\phi}$ are positive weighting scalars.

Upon solving for the optimal control trajectory $u^\star$, we employ only $u^\star(t_k)$ for $t \in (t_k, t_k + \tau_u]$ in accordance with MPC standard practice.

Note that in the nonlinear MPC formulation, the parameters N_p, N_u (number of control steps used in computing the predictive horizon), τ_u, and weights w_ℓ^{ϕ} and w_ℓ^u are design variables. We use $N_u = N_p$, and for all simulations, we choose

$$w_{\ell+1}^{\phi} = \ell + 1,$$
$$w_\ell^u = 0.001,$$

for $\ell = 0, \cdots, N_p - 1$.

Remark 6. Time-varying weights have been reported previously in the MPC literature and common software implementations; see, for example: Zheng [1997]; Bemporad et al. [2004]. In the manipulation of circadian rhythms, the use of increasing weights w_ℓ^{ϕ} ensures the computed control sequence $u^\star$ forces the controlled phase ϕ closer to the environmental phase ϕ_e for time steps toward the end of the predictive horizon. This embeds an implicit cost: to seek a control sequence that entrains quickly, without allowing the actual phase to deviate significantly from the environmental phase while allowing flexibility of the phase error near the start of the predictive horizon. Since it is not guaranteed that entrainment will occur within the selected predictive horizon N_p, we do not explicitly minimize the time to re-entrainment, preferring to include this information implicitly through a linearly increasing phase-error weighting term.

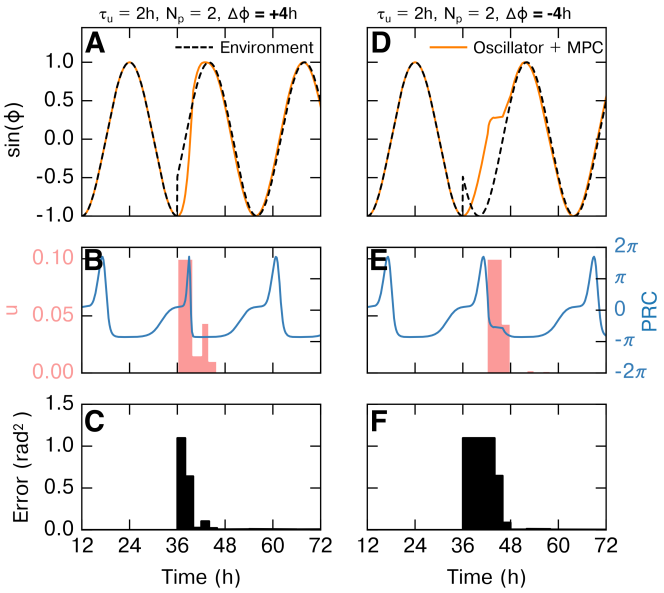

Fig. 2. Example of applying MPC to re-entrain the circadian oscillator following phase shifts of +4h (A-C) and -4h (D-F) applied at 12:00. (A, D) Sinusoidal representation of the phase of the environment (dashed) and the circadian clock under MPC (solid). A sinusoid is used to visualize the phase progression and avoid the complications of representing an 8-state oscillator. (B, E) Control inputs (u, shaded pink) and phase response curves (PRC, blue) for MPC examples. Because the positive phase shift in B occurs where the PRC is positive, the controller acts immediately. Despite a large error, the MPC is unable to correct the negative phase shift case in E until the PRC is negative, since the control variable is manipulated unidirectionally. (C, F) Phase difference (rad^2) between external and oscillator phase.

In the subsequent section, we demonstrate via simulation that N_p and τ_u cannot be chosen arbitrarily; careful consideration of the PRC of KL001 must be given in order to select N_p and τ_u for swift entrainment.

3. RESULTS

The Python programming language was used to formulate and solve the MPC problem. Specifically, packages CasADi (Andersson et al. [2012]), and SciPy were used to formulate the problem. The resulting optimization problem must be solved by nonlinear programming (NLP), as the cost function (8) and the predictor (5) are nonlinear. The optimal control input $u^\star$ was found by particle swarm via the PySwarm package.

3.1 Illustration of controller performance

To demonstrate the effectiveness of this approach, we solve the nonlinear MPC problem (8) to re-entrain the circadian oscillator following phase shifts of +4h ($\Delta\phi = \pi/3$) and -4h ($\Delta\phi = -\pi/3$) with $t_{\text{shift}} = 36$h (12:00 clock time), as shown in Fig. 2. For this preliminary test case, we used a controller time step of $\tau_u = 2$h and predictive horizon $N_p = 2$ steps. For a shift of +4h (Fig. 2A-C), the controller responds immediately to correct the shift, as it occurs in a positive region of the PRC. For the -4h shift, the controller immediately identifies only a positive PRC region and delays taking action until it reaches a region where the PRC is negative (Fig. 2E). This results in a larger accumulated error (Fig. 2F) than the negative shift case due to the delayed response, but ultimately the controller correctly identifies that a positive phase shift will not help re-entrain the clock.

Here, we are computing the control based on the phase-only formulation in (5) and applying $u(t_k)$ to the full 8-dimensional model from St. John et al. [2014]. Slight errors in predicted phase response may be caused by plant-model mismatch between the 8-state oscillator (here, the "plant") and the phase-only formulation of this oscillator used in calculating control inputs ("model"). These errors are the result of deviations from linear phase response behavior for oscillators not precisely on the limit cycle trajectory, where the linear phase response is calculated. These errors are small (notice a slight overshoot and correction following the initial controller action in Fig. 2A-C) and are rapidly corrected by the controller, as MPC is inherently robust to plant-model mismatch.

3.2 Importance of predictive horizon for entrainment performance

In the case of KL001 action, the PRC is asymmetric (see Fig. 1B): the area under the PRC for a negative phase shift is approximately twice that of the area under the PRC for a positive phase shift. Thus, a larger negative shift may be achieved in a single 24h cycle. If a 12h ($\pm\pi$) phase shift were applied at 12:00 clock-time with a short predictive horizon, the naive controller would choose to immediately apply a positive phase shift in order to reduce the difference between ϕ and ϕ_e, and it would take several cycles to re-entrain the clock with a positive 12h phase shift. If the predictive horizon were lengthened, the controller would correctly identify that the more optimal result would be to wait for the negative region of the PRC, and apply a single longer pulse to shift the clock back 12h in a single cycle. Thus, the ability of the controller to identify the correct control input is dependent carefully selecting the predictive horizon, N_p.

To demonstrate this effect, Fig. 3A-B show the MPC re-entrainment results for a 12h shift applied at 12:00 using predictive horizons of 4h (B, $\tau_u = 2$h, $N_p = 2$) and 24h (C, $\tau_u = 2$h, $N_p = 12$). Here, the sine of the phase of the oscillator and the environment are plotted, to reflect the mod 2π nature of phase. The $N_p = 2$ short horizon in Fig. 3A results in MPC phase-advancing a total of +12h over three cycles before it reaches re-entrainment. The $N_p = 12$ long horizon in Fig. 3B instead results in a single,

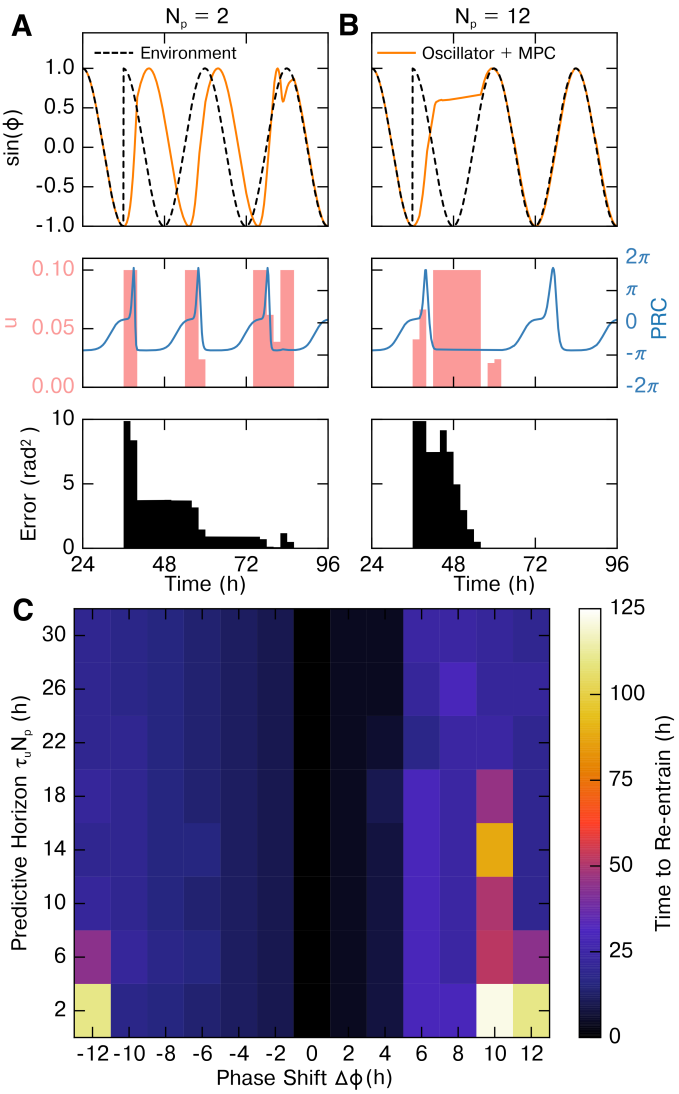

Fig. 3. Time to re-entrain following a phase shift is dependent on predictive horizon. Controller sampling time $\tau_u = 2$h is fixed at throughout. (A) For a 4h horizon, a 12h phase shift applied at 12:00 requires several days to re-entrain. Here, MPC uses several intermittent phase advances, as a phase advance is immediately available after the shift and the predictive horizon does not observe the larger phase delay region. (B) For a 24h horizon, the oscillator may be re-entrained in approximately 24h, as MPC identifies the optimal solution of applying a single, large dose of KL001 to cause a 12 hour phase delay. (C) A sweep across phase shift and predictive horizon demonstrates that a short predictive horizon may result in suboptimal re-entrainment of the circadian oscillator under MPC. The regions of suboptimal entrainment occur where the controller selects the incorrect direction to phase shift the clock, as in A and B.

sustained dose in the negative region of the PRC. Because this dose slows the phase progression, it also lengthens the negative region of the PRC, allowing a single, large dose to effect the full -12h shift in approximately 24h.

In Fig. 3C, we show the results of simulations for a range of phase shifts $\Delta\phi$ and predictive horizons N_p to identify

where MPC with a short predictive horizon results in slow re-entrainment. The time step $\tau_u = 2$h, and time of phase shift $t_{\text{shift}} = 36$h were held constant for all scenarios. This set of simulations was designed to explore regions in which MPC fails to find the shortest path to re-entrainment. Simulations were performed for $\Delta\phi \in \{-12, -10, \cdots, 12\}$ and $N_p \in \{1, 3, \cdots, 15\}$ to cover the full spread of possible phase shifts, and cover predictive horizons up to where re-entrainment time is unchanging.

Above a certain predictive horizon, in this case 22h ($N_p = 11$), the controller is able to correctly identify the most rapid path to re-entrainment. Thus, the time to re-entrain is constant for each $\Delta\phi$ for $N_p \geq 11$. For shorter predictive horizons, MPC fails to identify the optimal path to re-entrainment, particularly near the boundary where the time to re-entrain would be equal regardless of whether the controller selected to re-entrain through a phase advance or a phase delay. For this example, this boundary occurs near $\Delta\phi = +8$h (equivalent to -16 h), reflecting that there is approximately twice as much negative area under the PRC as positive area. For predictive horizons longer than 22h, all control trajectories are consistent.

3.3 Importance of controller sampling rate for entrainment

The sampling rate of the controller, τ_u, affects the time it takes the oscillator to entrain. Intuitively, as the control input is applied for the entire time step, a longer time step will necessarily result in a slower phase shift. A more interesting consequence of reducing sampling rate is that for sufficiently large τ_u, the controller may lose the ability to shift in one direction due to asymmetry of the PRC. Positive phase shifts are more sensitive to this phenomenon, as input in the positive region of a PRC will accelerate the oscillator through the positive region. Thus, a larger τ_u will effectively reduce the maximum control input which will still result in a positive phase shift, as a larger input will force the oscillator into a negative PRC region and reduce the magnitude of the net positive shift.

To specifically demonstrate this, Fig. 4A-B show MPC re-entrainment results for a 4h shift at 12:00 clock time, with a predictive horizon consisting of twelve 2h time steps (A) or two 12h time steps (B). In Fig. 4A, the controller is able to precisely target the most sensitive region of the PRC and re-entrain the oscillator in a single brief dose. In Fig. 4B, the dose is spread over a wider region including a region of negative phase response. Thus, the overall effect is lessened, and two doses are required for re-entrainment.

To identify where this phenomenon occurs, we performed simulations for a range of phase shifts $\Delta\phi$ and time steps τ_u. The total time of the predictive horizon $\tau_u N_p = 24$h, and time of phase shift $t_{\text{shift}} = 36$h were held constant for all scenarios. Simulations were performed for $\Delta\phi \in \{-12, -10, \cdots, 12\}$. Time step values $\tau_u \in \{1, 2, 3, 4, 6, 8, 12, 24\}$ were selected as the integer factors of the predictive horizon. The results of these simulations are shown in Fig. 4C. For four or more samples per 24h period ($\tau_u \leq 6$h), the time to re-entrain increases slightly with longer steps. For $\tau_u \geq 8$h (3 or fewer samples per 24h horizon), the controller shows reduced ability to re-entrain following short, positive phase shifts.

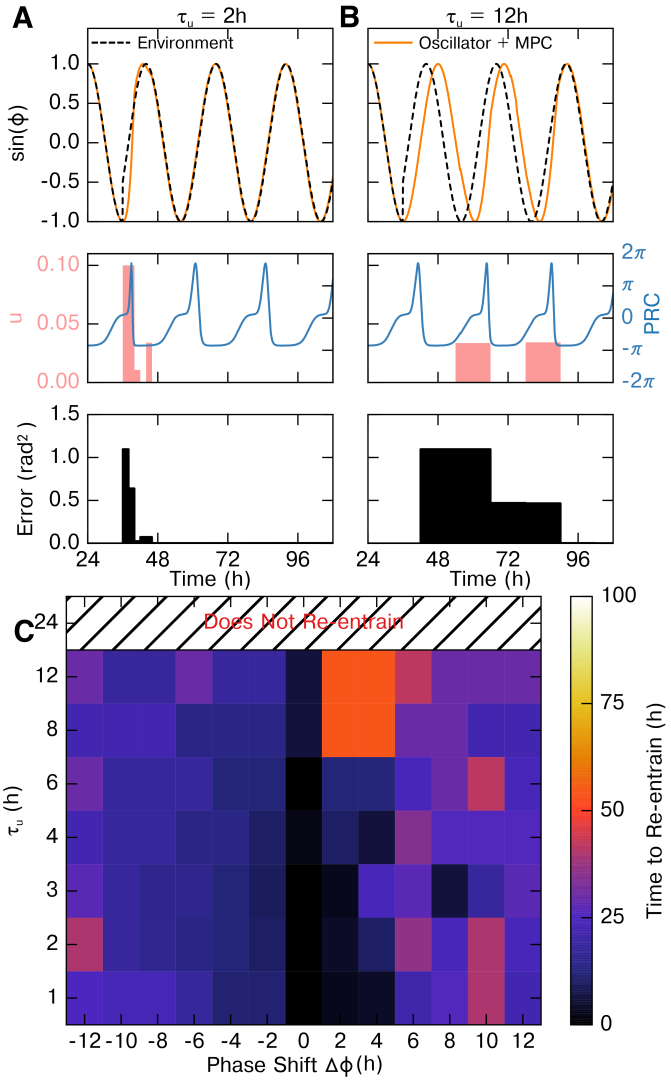

Fig. 4. Time to re-entrain following a phase shift is dependent on controller sampling rate and shape of the PRC. All predictive horizons are held constant at $\tau_u N_p = 24$h. (A) For $\tau_u = 2$h (12 samples per 24h horizon), re-entrainment to a +4h shift may occur rapidly, as the smaller positive PRC region can be targeted. (B) For $\tau_u = 12$h (two samples per 24h horizon), it takes multiple cycles to re-entrain, as each control step includes both a positive and negative PRC region. (C) A sweep across phase shift and sampling rate (predictive horizon $\tau_u N_p$ held constant at 24h) demonstrates that for a larger τ_u, the loss of resolution can result in a longer time to entrain. This is most explicitly evident for small positive phase shifts, as the positive region of the PRC is smaller and must be therefore more precisely targeted.

4. CONCLUSIONS

When designing an MPC approach for control of biological oscillators, one must ensure the sampling rate is sufficiently fast (sufficiently short τ_u) and the predictive horizon $\tau_u N_p$ is sufficiently long, otherwise the time required to phase-shift the clock may be suboptimal. The predictive horizon length and controller sampling rate which permit most rapid phase shifting are dependent upon the shape

of the PRC and thus must be evaluated individually for any potential therapeutic.

If multiple control targets are available, it may be advantageous to select a target or set of complementary targets providing similar areas under the positive and negative regions of the PRC in order to facilitate bidirectional phase shifting. The use of multiple control targets has been previously examined in Bagheri et al. [2008] with encouraging results. Biologically, multiple controls may result in shifting the oscillator far from the limit cycle trajectory during the course of the control.

One consequence of the restrictions on the control problem shown herein is that the pharmacokinetics of any potential therapeutic are also subject to these restrictions. For example, a controller time step much shorter than the half-life of the pharmaceutical would not make reasonable sense, as the system could not be controlled at this resolution. Similarly, if the half-life is significantly longer than the controller time step necessary for phase shifting, the effectiveness of the control will be greatly reduced. Future work will explicitly examine the role of pharmacokinetics on the ability to control these oscillators by incorporating pharmacokinetics into the model.

A more challenging question involves sensitivity of the PRC to uncertainty in kinetic parameters or variability in the *in vitro* measured PRC. Since MPC is naturally robust to plant-model mismatch, we expect the approach presented herein to perform reasonably well in the face of uncertainty. However, this necessitates additional study.

In this study we have used a model of the mouse circadian clock to approximate the phase response of a human. This approximation is reasonable, as the core clock function is largely conserved in mammals. However, future effort is necessary to determine the accuracy of this approximation, and the degree to which any circadian control algorithm should be personalized. There is a slight variability in circadian period between individuals (Kronauer et al. [1999]), and for large shifts these differences may become significant.

ACKNOWLEDGEMENTS

This work was funded by: National Institutes of Health (NIH) T32-HLO7901 (J.H.A.), and R01-GM096873-01 (F.J.D.).

REFERENCES

Abel, J.H. and Doyle III, F.J. (2016). A systems theoretic approach to analysis and control of mammalian circadian dynamics. *Chem. Eng. Res. Des.*, 116, 48–60.

Andersson, J., Akesson, J., and Diehl, M. (2012). *Recent Advances in Algorithmic Differentiation*, volume 87. Springer Berlin Heidelberg.

Bagheri, N., Stelling, J., and Doyle III, F.J. (2007). Circadian phase entrainment via nonlinear model predictive control. *Int. J. Robust Nonlinear Control*, 17(May), 1555–1571.

Bagheri, N., Stelling, J., and Doyle III, F.J. (2008). Circadian phase resetting via single and multiple control targets. *PLoS Comput. Biol.*, 4(7).

Bemporad, A., Morari, M., and Ricker, N.L. (2004). *Model Predictive Control Toolbox User's Guide*. The Mathworks, Inc.

Hirota, T., Lee, J.W., Lewis, W.G., Zhang, E.E., Breton, G., Liu, X., Garcia, M., Peters, E.C., Etchegaray, J.P., Traver, D., Schultz, P.G., and Kay, S.A. (2010). High-throughput chemical screen identifies a novel potent modulator of cellular circadian rhythms and reveals ck$i\alpha$ as a clock regulatory kinase. *PLoS Biol.*, 8(12), e1000559.

Hirota, T., Lee, J.W., St. John, P.C., Sawa, M., Iwaisako, K., Noguchi, T., Pongsawakul, P.Y., Sonntag, T., Welsh, D.K., Brenner, D.A., Doyle III, F.J., Schultz, P.G., and Kay, S.A. (2012). Identification of small molecule activators of cryptochrome. *Science*, 337(6098), 1094–1097.

Kronauer, R.E., Forger, D.B., and Jewett, M.E. (1999). Quantifying human circadian pacemaker response to brief, extended, and repeated light stimuli over the phototopic range. *J. Biol. Rhythms*, 14(6), 500–515.

Leloup, J.C. and Goldbeter, A. (2003). Toward a detailed computational model for the mammalian circadian clock. *Proc. Natl. Acad. Sci. U. S. A.*, 100, 7051–7056.

Marquié, J.C., Tucker, P., Folkard, S., Gentil, C., and Ansiau, D. (2015). Chronic effects of shift work on cognition: findings from the visat longitudinal study. *Occup. Environ. Med.*, 72(4), 258–264.

Mohawk, J.A., Green, C.B., and Takahashi, J.S. (2012). Central and peripheral circadian clocks in mammals. *Annu. Rev. Neurosci.*, 35(1), 445–462.

Serkh, K. and Forger, D.B. (2014). Optimal schedules of light exposure for rapidly correcting circadian misalignment. *PLoS Comput. Biol.*, 10(4), e1003523.

Shaik, O., Sager, S., Slaby, O., and Lebiedz, D. (2008). Phase tracking and restoration of circadian rhythms by model-based optimal control. *IET Syst. Biol.*, 2(1), 16–23.

Slaby, O., Sager, S., Shaik, O.S., Kummer, U., and Lebiedz, D. (2007). Optimal control of self-organized dynamics in cellular signal transduction. *Math. Comput. Model. Dyn. Syst.*, 13(5), 487–502.

St. John, P.C., Hirota, T., Kay, S.A., and Doyle III, F.J. (2014). Spatiotemporal separation of per and cry posttranslational regulation in the mammalian circadian clock. *Proc. Natl. Acad. Sci. U. S. A.*, 111(5), 2040–2045.

Taylor, S.R., Doyle III, F.J., and Petzold, L.R. (2008a). Oscillator model reduction preserving the phase response: application to the circadian clock. *Biophys. J.*, 95(4), 1658–1673.

Taylor, S.R., Gunawan, R., Petzold, L.R., and Doyle III, F.J. (2008b). Sensitivity measures for oscillating systems: Application to mammalian circadian gene network. *IEEE Trans. Automat. Contr.*, 53, 177–188.

Zhang, J., Qiao, W., Wen, J.T., and Julius, A. (2016). Light-based circadian rhythm control: Entrainment and optimization. *Automatica*, 68, 44–55.

Zheng, A. (1997). Stability of model predictive control with time-varying weights. *Comput. Chem. Eng.*, 21(12), 1389–1393.